

DETECTION OF DIELECTRIC CONTRAST OF BREAST TISSUES USING CONFOCAL MICROWAVE TECHNIQUE

G. Bindu,¹ Santhosh John Abraham,² Anil Lonappan,¹ Vinu Thomas,¹ C. K. Aanandan,¹ and K. T. Mathew¹

¹ Department of Electronics
Microwave Tomography and Materials Research Laboratory
Cochin University of Science and Technology
Kochi-682 022, India

² Department of Surgery
Lourde Hospital
Kochi, India

Received 9 December 2005

ABSTRACT: Confocal microwave technology is explored as a screening tool to detect regions of dielectric contrast in breast tissues. When exposed to microwaves, malignant breast tissues exhibit electrical properties that are significantly different from that of healthy breast tissues, due to the variations of bound water content. In vitro studies of normal breast tissues having cancerous inclusions in the presence of a matching coupling medium are reported here. Experimentally obtained time-domain results are substantiated by finite-difference time-domain analysis. It is observed that the dielectric contrast of breast tissues is satisfactorily determined using the pulsed confocal microwave technique. © 2006 Wiley Periodicals, Inc. *Microwave Opt Technol Lett* 48: 1187–1190, 2006; Published online in Wiley InterScience (www.interscience.wiley.com). DOI 10.1002/mop.21570

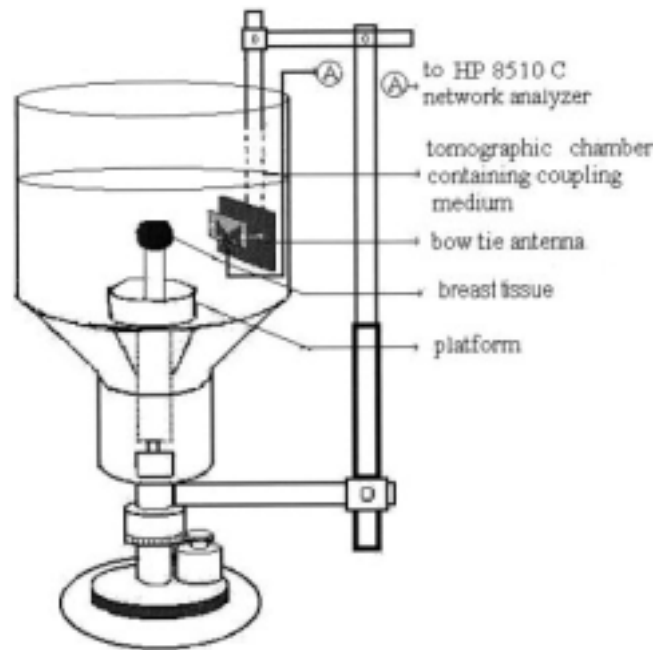
Key words: confocal microwave technique; breast tumors; dielectric permittivity; FDTD method

INTRODUCTION

Breast cancer affects many women and early detection aids in fast and effective treatment. X-ray mammography is currently the most effective imaging method for detecting clinically occult breast cancer. However, despite significant progress in improving mammographic techniques for detecting and characterizing breast lesions, mammography reported high false-negative rates [1] and high false-positive rates [2]. The association of X-ray mammography with uncomfortable or painful breast compression and exposure to low levels of ionizing radiation may reduce patient compliance with screening recommendations. These concerns augment the search for techniques that image other physical tissue properties or metabolic changes.

The motivation for developing a microwave technique for detecting breast cancer is the significant contrast in the dielectric properties of normal and malignant breast tissues at microwave frequencies [3]. Further more, microwave attenuation in normal breast tissue is low enough to make signal propagation feasible, even through large breast volumes. In addition, microwave technology is noninvasive and nonionizing, and eliminates uncomfortable breast compression. These reasons make microwave technology a promising technique for the detection of biological anomalies such as breast cancer. The small size and physical accessibility of the breast compared to other internal organs is also an added advantage.

When exposed to microwaves, the high water content of malignant breast tumors causes significantly large microwave scattering compared to normal fatty breast tissues that have low water content. It is reported that the increase of dielectric permittivity and conductivity for cancerous breast tissue is twice or more than that of the host tissue [4].



Measurement set up

Figure 1 Measurement setup

Versions of video pulse radars were introduced for medical applications as a means to detect malignancy in internal biological tissues [5]. Confocal microwave technology (CMT), employing a short-pulse, wide band-pass, backscattering technique to locate early stage breast tumors, is a topic of interest of many researchers [6]. In contrast to X-ray mammography, the nonionizing CMT exploits the translucent nature of the breast and obtains a large dielectric contrast of the tissues according to their water content. Moreover, CMT avoids complex image reconstruction algorithms. As the illuminating signal is wide band, simple time-shifting and summing of the signals are enough to detect the malignant tissues.

This paper presents the application of pulsed CMT for the detection of regions of dielectric contrast of breast tissues.

MODELS

System Configuration

The schematic diagram of the experimental setup is shown in Figure 1. It consists of a chamber of radius 12 cm and height 30 cm, coated inside with a suitable absorbing material. A single suspended bowtie antenna is used for both transmission and reception of microwave energy. The breast-tissue samples are supported on a cylindrical low-loss PVC holder ($\tan\delta = 0.0002$ and $\epsilon_r = 2.1$, when measured at 3 GHz) of radius 1 cm, placed at the center of the measurement setup. The sample and the antenna are immersed in a matching coupling medium to minimize the reflections and to improve the resolution.

All measurements are done using an HP 8510 C network analyzer interfaced with workstation.

Wideband Antenna

A coplanar strip-line-fed bowtie antenna generating the TM_{01} mode is designed for both transmission and reception of microwave energy. As CMT is a time-domain approach, bandwidth is

TABLE 1 Results at 2.983 GHz

Sample		Dielectric Permittivity	Conductivity [S/m]	Bound Water Content [%]
Breast tissue, patient 1 (age 47)	Normal	20.43	3.12	43
	Cancerous	32.31	3.52	62
Breast tissue, patient 2 (age 49)	Normal	18.85	2.71	42
	Cancerous	38.73	4.12	65
Breast tissue, patient 3 (age 51)	Normal	24.98	3.25	45
	Cancerous	40.1	4.31	65
Breast tissue, patient 4 (age 45)	Normal	19.5	2.64	41
	Cancerous	30	3.34	61
Corn syrup		18.7	0.64	NA

the major deciding factor in the antenna design. The experimental investigation [7] shows that the designed antenna exhibits enhanced 2:1 VSWR bandwidth of ~46% in the operational band of 1850–3425 MHz. This result complements the FDTD computed bandwidth of 52% [8] in the operational band of 1725–3575 MHz.

Samples

Samples of breast tissues of the same person were collected from Department of Surgery, Lourde Hospital, Kochi and subjected to study within 30 min of mastectomy. Four cases were studied: (i) A cancerous breast tissue of ~0.5-cm radius inserted in normal breast tissue of ~1-cm radius of patient 1, is taken as B-sample 1; (ii) four tumorous inclusions of ~0.25-cm radius each inserted in normal tissue of ~1-cm radius of patients 2 and 3 are treated as B-samples 2 and 3; (iii) scattered inclusions of cancerous tissue of ~0.1-cm radius each inserted in normal tissue of ~1-cm radius of patient 4 is treated as B-sample 4.

Coupling Medium

Corn syrup of permittivity 18.7 and conductivity 0.64 S/m is selected as the coupling medium for the study [9]. To check the feasibility of using this sample as the coupling medium, dielectric studies of breast tissues used have been done using the rectangular-cavity perturbation method [10]. The results obtained at 2.983 GHz are tabulated in Table 1. This frequency is selected as it is the nearest resonant frequency of the rectangular cavity to the resonant frequency of the antenna. The results are in good agreement with the available literature data on breast tissues [11].

It is observed that corn syrup exhibits a good permittivity match with that of the normal breast tissue, while having lesser conductivity. This ensures good coupling of electromagnetic energy in to the tissue with less propagation loss.

METHODS

Data Acquisition

To acquire data, the tissue sample is illuminated by the wideband bowtie antenna and the same antenna collects the back-scattered waves. The antenna is rotated around the sample at a radius of 6 cm and measurements are taken for every 10° position of the antenna. A time-shift-and-add algorithm is applied to the set of recorded pulses to enhance the returns from high-contrast regions and reduce clutter. This involves computing the time delay for the roundtrip between each antenna position to a point in the domain of interest, then adding the corresponding portions of the time signals recorded at each antenna position.

FDTD Analysis

To validate the experimental investigation, the theoretical analysis is done using the finite-difference time-domain (FDTD) method. The dispersive nature of the dielectric medium is incorporated in the constitutive FDTD equations using the 1st-order Debye dispersion relation [12, 13]. The geometry under consideration consists of an infinitely long multilayered cylinder of dispersive dielectric nature with its axis in the z direction. The incident wave is assumed to be + y -directed plane wave whose electric-field vector is in the z direction. Because there is no variation of either the scatterer geometry or incident fields in the z direction, this problem is treated as a 2D scattering of the incident wave with only E_z , H_x , and H_y fields present. The electric and magnetic fields in a non-magnetic medium are given by

$$H_x(i, j, t + 1) = H_x(i, j, t) - \frac{dt}{\mu_0 dy} (E_z(i, j, t) - E_z(i, j - 1, t)), \quad (1)$$

$$H_y(i, j, t + 1) = H_y(i, j, t) - \frac{dt}{\mu_0 dx} (E_z(i, j, t) - E_z(i - 1, j, t)), \quad (2)$$

$$E_z(i, j, t + 1) = \frac{\epsilon_\infty}{\epsilon_\infty + \chi_0(i, j)} E_z(i, j, t) + \frac{1}{\epsilon_\infty + \chi_0(i, j)} \sum_{m=0}^{t-1} E_z(i, j, t - m) \Delta \chi_m(i, j) + \frac{dt}{\epsilon_\infty + \chi_0(i, j) \epsilon_0 dx} (H_y(i + 1, j, t) - H_y(i, j, t)) - \frac{dt}{\epsilon_\infty + \chi_0(i, j) \epsilon_0 dy} (H_x(i, j + 1, t) - H_x(i, j, t)), \quad (3)$$

where

$$\chi_0(i, j) = (\epsilon_s - \epsilon_\infty)(1 - \exp(-dt/t_0)) \quad (4)$$

is the susceptibility function, and

$$\Delta \chi_m(i, j) = (\epsilon_s - \epsilon_\infty)(\exp(-mdt/t_0)(1 - \exp(-dt/t_0))^2, \quad (5)$$

where ϵ_s is the static permittivity, ϵ_∞ is optical permittivity and t_0 is the dielectric relaxation time. A Gaussian pulse of half-width T as 18 ps with the time delay t_o of 54 ps is selected as the source of excitation. Space steps of 0.1 cm and time steps of 6.05 ps are chosen to ensure propagation of the waves in the entire domain. Mur's 2nd-order absorbing boundary conditions are applied to terminate the FDTD grid.

RESULTS AND DISCUSSIONS

Figure 2 shows the time-domain response of B-sample 1. Here, peaks A and D in the encircled region represent reflections from the coupling medium–normal tissue interface. As the dielectric contrast is less here, the reflections are less compared to the reflections produced by the cancerous tissues. Peaks B and C correspond to reflections from the tumor inclusions. It is observed that peak C exhibits lesser amplitude compared to B. This is due to the fact that strength of the reflected signal decreases with distance of propagation. The experimental and FDTD results show

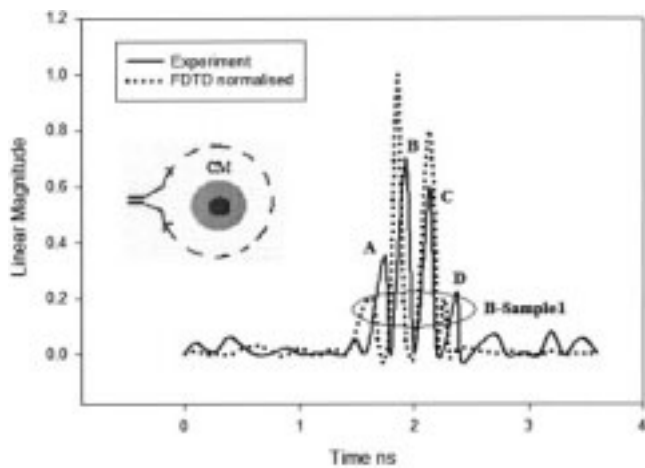


Figure 2 Time-domain responses of B-sample 1 (of patient 1)- single cancerous tissue of ~ 0.5 -cm radius inserted in normal tissue of ~ 1 -cm radius (of patient 1). □ Normal tissue; ■ cancerous tissue; CM: coupling medium

good agreement, as there is only a single tumor inclusion in B-sample 1.

Figures 3–5 show the time-domain responses of B-samples 2–4. In all the figures, the first and the last peaks in the encircled region represent reflections from the normal breast tissue and the remaining peaks are reflections from the tumorous inclusions. The FDTD and experimental results do not agree well in these figures due to the presence of multiple inclusions. Reflections from nearby contrast points overlap and are represented as a single point. The time-shift-and-add algorithm applied to the experimental data causes the reflected signals from tumors located opposite each other to overlap. Even though exact tumor locations are difficult to figure, regions of dielectric contrast are satisfactorily detected using this time-domain confocal microwave technique. The amplitudes of the tumor reflections B in Figures 3 and 4 are higher than those in Figures 2 and 5 due to the higher dielectric permittivities of the cancerous tissues in B-samples 2 and 3 compared to those in B-samples 1 and 4.

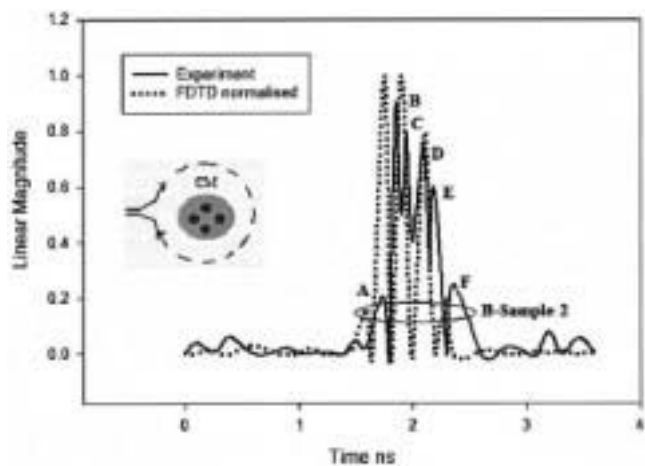


Figure 3 Time-domain responses of B-sample 2 (of patient 2): four tumorous inclusions of ~ 0.25 -cm radius each, inserted in normal tissue of ~ 1 -cm radius. □ Normal tissue; ■ cancerous tissue; CM: coupling medium

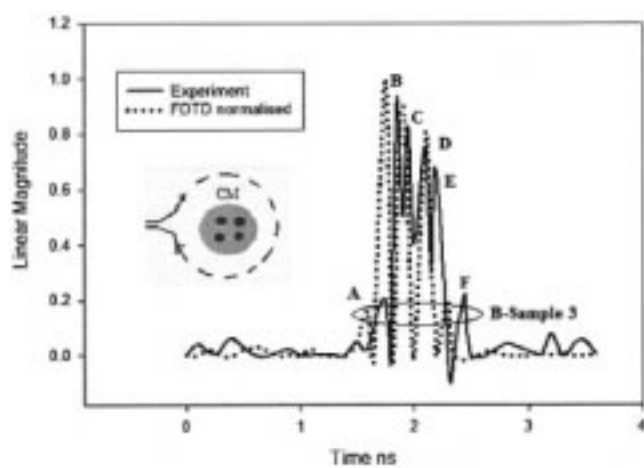


Figure 4 Time-domain responses of B-sample 3 (of patient 3): four tumorous inclusions of ~ 0.25 -cm radius each, inserted in normal tissue of ~ 1 -cm radius. □ Normal tissue; ■ cancerous tissue; CM: coupling medium

A time gating of 9.032 ns is provided from the network analyzer to enhance the backscatter detection while suppressing clutter. The calibration of the system was performed in the absence of the breast tissues.

The bound water contents of the breast tissue samples were determined by subjecting 10 gm of each of the sample in a preheated oven at 70°C until the weights of the samples were reduced to 1 gm. The heating time of the samples was varied from 5 to 7 s. The bound water contents of the breast samples are shown in Table 1. The variations of dielectric parameters of the samples are attributed to this variation of bound water content.

Approximate tumor locations with respect to the tallest peak in Figures 2–5 are calculated from the following equation. The velocity of propagation depends on the dielectric permittivity of the medium, given by

$$v = \frac{2d}{t}, \quad (6)$$

where

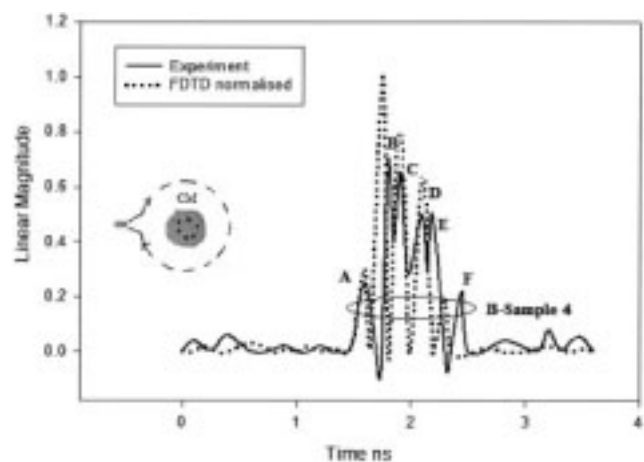


Figure 5 Time-domain responses of B-sample 4 (of patient 4): scattered tumorous inclusions of ~ 0.1 -cm radii each inserted in normal tissue. □ Normal tissue; ■ cancerous tissue; CM: coupling medium

TABLE 2 Approximate Tumor Locations with Respect to the First Tumorous Inclusion in Figs. 2–5 (With Respect to the Tallest Peak in Time-Domain Graphs)

B-sample	Actual Distance of Nearest Tumorous Inclusion from the Antenna [cm]	Approximate Distance Calculated from Experimental Time-Domain Data [cm]
1	6	6.38
2	6	6.16
3	6	6.23
4	6	6.21

$$v = \frac{c}{\sqrt{\epsilon_r}}, \quad (7)$$

d is the distance, t is the time taken for propagation, ϵ_r is the dielectric permittivity of the medium, and c is the velocity of light. The results are tabulated in Table 2 and good agreement is observed.

CONCLUSION

The confocal microwave technique has been studied as a screening tool to detect regions of dielectric contrast of breast tissues. Normal and malignant breast tissues exhibit considerable difference in the dielectric properties due to the variations in bound water content. In vitro studies of normal breast tissues having cancerous inclusions in the presence of a matching coupling medium show that dielectric contrast of breast tissues can be accurately determined using the pulsed confocal microwave technique. Hence the method can be used for early stage detection of breast cancer.

ACKNOWLEDGMENT

Authors G. Bindu and Anil Lonappan thankfully acknowledge Council of Scientific and Industrial Research, Govt. of India for providing Senior Research Fellowships.

REFERENCES

1. P.T. Huynh, A.M. Jarolimek, and S. Dayee, The false-negative mammogram, *Radiographics* 18 (1998), 1137–1154.
2. J.G. Elmore, M.B. Barton, V.M. Mocerri, S. Polk, P.J. Arena, and S.W. Fletcher, Ten year risk of false positive screening mammography and clinical breast examinations, *New England J Medicine* 338 (1998), 1089–1096.
3. E.C. Fear, S.C. Hagness, P.M. Meaney, M. Okoniewski, and M.A. Stuchly, Enhancing breast tumor detection with near field imaging, *IEEE Microwave Mag* 3 (2002), 48–56.
4. S.S. Chaudhary, R.K. Mishra, A. Swarup, and J.M. Thomas, Dielectric properties of normal and malignant human breast tissues at radiowave and microwave frequencies, *Indian J Biochem Biophys* 21 (1981), 76–79.
5. J.D. Young, L. Peters, Jr., Examination of video pulse radar systems as potential biological exploratory tools, L.E. Larson and J.H. Jacobi (Eds.), *Medical applications of microwave imaging*, IEEE Press New York, 1986, pp. 82–105.
6. S.C. Hagness, A. Taflov, and J.E. Bridges, Three-dimensional FDTD analysis of a pulsed microwave confocal system for breast cancer detection: design of an antenna-array element, *IEEE Trans Antennas Propagat* 147 (1999), 783–791.
7. G. Bindu, V. Hamsakutty, A. Lonappan, J. Jacob, V. Thomas, C.K. Aanandan, and K.T. Mathew, Wideband bowtie antenna with coplanar stripline feed, *Microwave Opt Technol Lett* 42 (2004), 222–224.
8. G. Bindu, A. Lonappan, C.K. Aanandan, and K.T. Mathew, Wideband bowtie antenna for confocal microwave imaging, *Asia-Pacific Microwave Conf*, New Delhi, 2004. APMC'04.

9. G. Bindu, A. Lonappan, V. Thomas, V. Hamsakutty, C.K. Aanandan, and K.T. Mathew, Microwave characterization of breast phantom materials, *Microwave Opt Technol Lett* 43 (2004), 506–508.
10. K.T. Mathew and Raveendranath, U. *Sensors Update*, Wiley–VCH, Germany, 1999, pp. 185–210.
11. A.M. Campbell and D.V. Land, Dielectric properties of female human breast tissue measured in vitro at 3.2 GHz, *Phys Medicine Biol* 37 (1992), 193–210.
12. P. Kosmas, C.M. Rappaport, and E. Bishop, Modeling with the FDTD method for microwave breast cancer detection, *IEEE Trans Microwave Theory Tech* 52 (2004), 1890–1897.
13. R. Luebbers, F.P. Hunsberger, K.S. Kunz, R.B. Standler, and M. Schneider, A frequency dependent finite-difference time domain formulation for dispersive materials, *IEEE Trans Electromagn Compat* 32 (1990), 222–227.

© 2006 Wiley Periodicals, Inc.

A DIRECTIVITY-DIVERSITY MICROSTRIP ANTENNA ARRAY IN MILLIMETER WAVE

M. Caillet, O. Lafond, M. Himdi, and L. Le Garrec

Institut d'Electronique et Télécommunications de Rennes (IETR)
UMR CNRS 6164
Université de Rennes I
35042 Rennes Cedex, France

Received 13 December 2005

ABSTRACT: The purpose of this paper is to report on a microstrip reconfigurable antenna in the millimeter-wave range. This antenna has directivity diversity and is based on a four-element array. An original method is outlined to guarantee matching for each configuration without changing circuit. Great results have been achieved with a passive prototype and an active antenna is under consideration. © 2006 Wiley Periodicals, Inc. *Microwave Opt Technol Lett* 48: 1190–1194, 2006; Published online in Wiley InterScience (www.interscience.wiley.com). DOI 10.1002/mop.21569

Key words: millimeter-wave antennas array; antenna radiation patterns; microwave switches; road vehicles

1. INTRODUCTION

Reconfigurable antennas have recently received a lot of attention [1–9] due to their ability to have diversity in radiation pattern, polarization, and frequency (and sometimes two or three diversities with the same antenna). A microstrip smart antenna is an extremely attractive candidate for obtaining reconfigurable characteristics due to its advantages of low profile, light weight, conformability, and (especially) ease of fabrication and integration with RF devices. Several solutions have been shown to obtain the antenna diversity: for example, a slot has been included in the patch [7] so as to change the resonant frequency, and a Vee-antenna permit to steer the radiation beam or change the shape of the beam using electrically-controlled microactuators [3]. All these solutions require an RF-switch or actuator, as active components or MEMS.

Antenna diversities have shown strong potential in wireless communications [10, 11] and have been studied extensively in the microwave range. Interest in reconfigurable antennas operating in the millimeter-wave range is currently emerging in various areas: typical planned applications include automotive radar, house automation, and so forth. Most of the time, the frequency and the